

Interactive influences of iron and light limitation on phytoplankton at subsurface chlorophyll maxima in the eastern North Pacific

Brian M. Hopkinson¹ and Katherine A. Barbeau

Geosciences Research Division, Scripps Institution of Oceanography, University of California–San Diego, 9500 Gilman Drive, La Jolla, California 92093-0218

Abstract

The roles of iron and light as limiting and colimiting factors for phytoplankton growth in subsurface chlorophyll maxima (SCMs) were investigated in mesotrophic to oligotrophic waters of the Southern California Bight and the eastern tropical North Pacific using microcosm manipulation experiments. Phytoplankton responses indicative of iron–light colimitation were found at several SCMs underlying macronutrient-limited surface waters in the eastern Pacific. Iron additions led to a shift in the size and taxonomic structure of the phytoplankton community, where large diatoms dominated what was formerly a diverse community of relatively small phytoplankton. The strongest and most ubiquitous responses of diatoms to iron addition were found under elevated light conditions, indicating that iron availability may have the greatest potential to affect SCM phytoplankton communities when light levels increase rapidly, such as during eddy events or with strong internal waves. The results show that iron influences phytoplankton community structure at SCMs, which would have consequences for nutrient cycling and carbon export within the lower euphotic zone.

It is now well established that iron can control phytoplankton biomass and productivity in high nutrient–low chlorophyll (HNLC) regions, where unused macronutrients are persistently present in surface waters. More recently, the importance of iron availability for phytoplankton has been shown in waters outside of HNLC areas. In coastal upwelling zones, rapid movement of high-macronutrient waters into the well-lit surface layer results in iron limitation when no supplemental iron sources from continental shelf or riverine inputs are available (Hutchins et al. 1998). Such conditions are common off the dry, steep coastlines that characterize major upwelling areas along the coasts of western North and South America, leading to frequent iron limitation in these waters (Hutchins et al. 1998, 2002). In the tropical North Atlantic, nitrogen generally limits phytoplankton growth, but iron, along

with phosphorus, limits the rate of nitrogen fixation and therefore indirectly constrains phytoplankton biomass (Mills et al. 2004). It has been speculated that iron may be an important control on nitrogen fixation throughout the oceans due to the high iron requirement of nitrogenase, the key enzyme responsible for the conversion of N₂ to ammonia.

While the nitrogenase enzyme is a significant iron demand for nitrogen fixers, for most photosynthetic organisms, the primary use of iron is in photosynthetic proteins (Raven 1990). In marine phytoplankton, recent measurements of iron allocation in the diatoms *Thalassiosira weissflogii* and *Thalassiosira oceanica* have shown that nearly all cellular iron is localized in photosynthetic light-harvesting and electron-transport proteins under low-iron conditions (Strzepek and Harrison 2004). This may be true for many phytoplankton taxa, as suggested by the increased iron quotas and lowered iron-use efficiencies observed in other diatom and dinoflagellate species in response to decreased light levels (Sunda and Huntsman 1997). The increased iron requirements at lower light provide evidence that photosynthetic needs dictate iron quotas, and for *T. weissflogii* and *T. oceanica*, it has been demonstrated that this is the case (Strzepek and Harrison 2004). The observation that iron requirements increase as light decreases, likely driven by photosystem requirements, has led to the hypothesis that phytoplankton may be colimited by iron and light in low-light environments (Sunda and Huntsman 1997). In an iron–light colimited state, growth and photosynthesis are ultimately limited by light processing, but production of photosynthetic proteins required to harvest and process light is constrained by iron availability (Fig. 1). It has been hypothesized that iron–light colimitation may occur in low-iron regions with deep mixed layers, such as the Southern Ocean, or even in macronutrient-limited, stratified waters, near the base of the euphotic zone (Sunda and Huntsman 1997).

¹Present address: Department of Geosciences, Princeton University, Princeton, New Jersey, 08544.

Acknowledgments

We thank Ralf Goericke, chief scientist of the R/V *New Horizon* and R/V *Roger Revelle* cruises, for letting us participate in the cruises, assistance with phytoplankton pigment analysis, loan of the pulse amplitude–modulated (PAM) fluorometer, and for valuable comments on this manuscript. Chief scientist Mike Landry was of great help on the R/V *Knorr* cruise. Andrew King, Chris Dupont, and Sue Reynolds provided assistance on cruises. We also thank the captain and crew of each vessel for their assistance. Andrew King analyzed several iron samples reported in this paper using his flow-injection analysis system. Support and supplementary data from the California Current Ecosystem Long-Term Ecological Research (LTER) program and the California Cooperative Oceanic Fisheries Investigations (CalCOFI) programs made this work possible. Helpful comments from Philip Boyd and two anonymous reviewers improved the manuscript. This research was funded by National Science Foundation (NSF) grants (OCE-0220959, OCE-0550302, LTER-0417616 to K.B.) and a National Defense Science and Engineering Graduate fellowship to B.H.

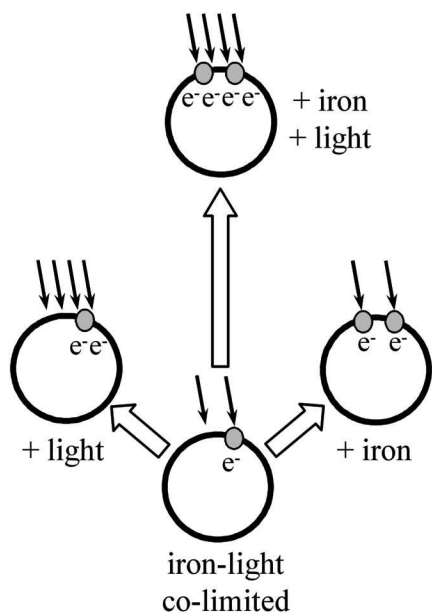


Fig. 1. Conceptual model of iron–light colimitation of phytoplankton growth rate due to iron requirements of the photosynthetic system (Sunda and Huntsman 1997). In this state, the ability to process light limits energy generation (represented by electrons: e^-) and growth, while the availability of iron limits production of photosynthetic proteins (gray ovals in cell membrane) used to process light. Increasing iron or light (angled, solid arrows) individually would be expected to increase growth rate, and a synergistic effect should be observed if both variables are increased together.

Field research into interactions between iron and light availability has primarily focused on classic HNLC regions in the subarctic North Pacific and the Southern Ocean. Experiments in these regions have shown that limitation or colimitation by iron and light depend on the local environmental conditions, and high-latitude HNLC regions should not be thought of as exclusively iron limited. An example of iron–light colimitation was found during the winter in the subarctic North Pacific, where a deep mixed layer (80 m), low incident irradiance, and lack of available iron combined to limit photosynthesis and maintain low phytoplankton biomass (Maldonado et al. 1999). In the region of the Subantarctic Front, it was determined that iron limited growth in an area with a relatively shallow (40 m) mixed layer, but light, in conjunction with iron, controlled growth in an area with deeper (90 m) mixed layers (Boyd et al. 2001). Iron–light colimitation has also recently been shown to be a factor influencing phytoplankton growth during the North Atlantic spring bloom (Moore et al. 2006). While these studies show that iron–light interactions are likely important to consider in high-latitude regions with deep mixed layers, there have been no field experiments to assess the potential effect of iron–light colimitation in the lower euphotic zone in stratified, macronutrient-limited waters.

The surface mixed layer is the most accessible stratum of the ocean, both to ships and satellites, and it is often the most productive layer of water columns, but important

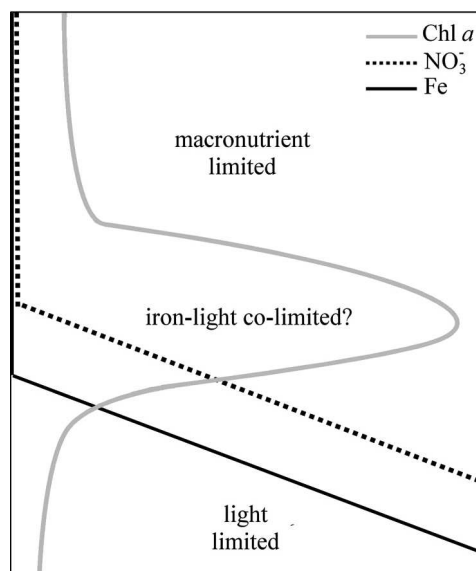


Fig. 2. SCMs are formed at the interface of the light-limited and macronutrient-limited regions of the water column. It was hypothesized that iron–light colimitation may occur at the top of the nitracline where nitrogen stress is relieved, but light is low, resulting in high photosynthetic iron requirements. The relationship between the ferricline and nitracline is also an important factor generating iron stress at these depths in the water column. The ferricline is frequently deeper than the nitracline, as diagrammed here, though in some water columns, they are coincident (Johnson et al. 1997b).

biological processes occur within the lower euphotic zone. Through vertical transport mechanisms, new nutrients are introduced and first biologically utilized in the lower euphotic zone, and so ecosystem processes within this layer can affect the fate of newly available nutrients as they are transported toward surface waters. In many water columns, the lower region of the euphotic zone is characterized by a subsurface chlorophyll maximum, generally a site of high phytoplankton biomass and productivity, and carbon export (Cullen 1982; Coale and Bruland 1987). Subsurface chlorophyll maxima (SCMs) are generated at the interface of the nutrient- and light-limited portions of the water column, and phytoplankton growth within a subsurface chlorophyll maximum is sensitive to adequate acquisition of both light and nutrients (Fig. 2.; Cullen 1982; Fennel and Boss 2003). SCMs have been identified in both macronutrient- and iron-limited regions, and they are a general feature of water columns in which the limiting nutrient is predominately supplied from below at a modest rate, though multiple factors contribute to their formation and evolution (Parslow et al. 2001)

Knowing the physiological link between iron availability and photosynthesis, we sought to investigate the significance of iron and light as limiting and colimiting factors within SCMs. Although nitrate is likely to limit growth in the upper portions of the SCM, we suspected that iron may be an important factor deeper in the SCM as light levels decrease and nitrate levels increase, relieving nitrogen stress but exacerbating iron demands (Fig. 2). Iron may be especially scarce in this layer when the ferricline is deeper

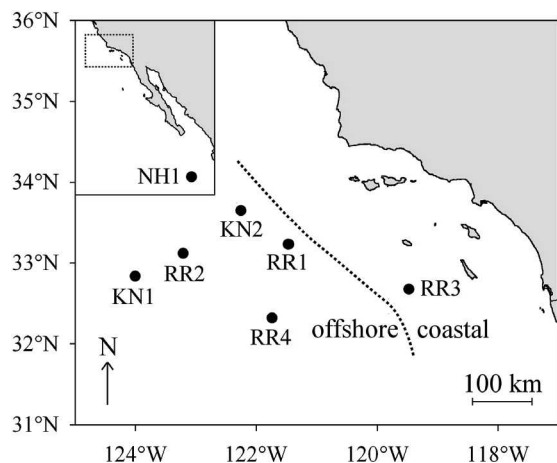


Fig. 3. A map of the Southern California Bight region where most of the incubations were initiated, an inset map of the northeast Pacific showing the location of NH1 (17°24'N, 108°17'W), and a dotted box around the southern California Bight region. The dotted line in the main map indicates the approximate location of the coastal/offshore boundary coinciding with the inshore edge of the California Current. The boundary was defined based on chlorophyll variability (Hayward and Venrick 1998) and is consistent with patterns in phytoplankton floristics (Venrick 1998). Although this boundary is based on surface characteristics, it is in part the result of subsurface processes and generally corresponds to the point where a stronger inshore shoaling of the nitracline begins (Hayward and Venrick 1998). This boundary is variable depending on the flow of the California Current, and it should be noted that RR1 was initiated at a time of higher productivity from waters more characteristic of the coastal regime.

than the nitracline, as is frequently observed (Johnson et al. 1997a,b). Microcosm experiments in which iron and light levels were manipulated were conducted in the Southern California Bight and the eastern tropical North Pacific. These experiments were used primarily to understand factors that limit the growth rate and abundance of various phytoplankton in SCMs, but they may also provide information on the effect of iron and light perturbations on SCM communities. An analysis of community responses to changes in light and iron levels suggested that iron–light colimitation of growth rate may be occurring in certain SCMs. In all experiments, significant effects of iron were observed when light limitation was relieved. These results also provide insight into the likely response of SCM

communities to changes in iron or light availability due to dust inputs of iron, or variability in light levels from doming of isopycnals by upwelling eddies or changes in cloud cover.

Methods

Incubation setup—Incubation experiments were conducted on two cruises in the Southern California Bight (SCB) in November of 2004 aboard the R/V *Roger Revelle* (incubations denoted RR) and May of 2006 aboard the R/V *Knorr* (KN incubations), and in the eastern tropical North Pacific (ETNP) on an R/V *New Horizon* cruise in November of 2003 (NH incubation). Locations in the SCB and ETNP where waters were collected for incubation experiments are shown in Fig. 3. At each station, water was collected using 12- or 30-liter trace-metal-clean GO-Flo bottles attached to a nonmetallic line. Depths for water collection were chosen based on water-column profile data obtained from a conductivity-temperature-depth (CTD) cast immediately prior to the GO-Flo cast. The top of the nitracline (1–6 $\mu\text{mol L}^{-1} \text{NO}_3^-$) within the SCM was targeted as a likely region to find iron stress, since nitrogen limitation was not expected to occur in this layer, and light levels were low but still high enough to support phytoplankton growth. Once recovered on deck, GO-Flo bottles were pressurized with 0.4- μm -filtered, ultrahigh-purity nitrogen gas, and water was dispensed within a class-100 laminar-flow bench into acid-washed 2.7- or 4-liter polycarbonate incubation bottles through acid-cleaned Teflon tubing without pre-screening. Multiple 12-liter GO-Flo bottles were required to set up a single incubation, in which case, incubation bottles were filled equally from each GO-Flo bottle to ensure uniform initial conditions. Incubations were conducted either in shaded, flow-through, on-deck incubators, or, indoors, in a temperature-controlled incubator set to 14°C to approximate in situ temperatures (13–14°C) (Table 1). When placed in the flow-through incubators, bottles were sealed in plastic bags to prevent trace-metal contamination.

Iron and light manipulations—Filled incubation bottles were randomly assigned in duplicate to the four experimental treatments: control (C), added iron (+Fe), increased light (+L), and added iron and increased light (+Fe+L). Five nmol L^{-1} iron additions were made during incubation

Table 1. Incubation initial conditions, depth from which incubations were collected and initial water properties are reported, and light conditions in situ and during incubation (as percent surface irradiance). Most of the incubations were conducted in an indoor incubator (In), although some were conducted in on-deck flow-through incubators (Out).

Incubation	Depth (m)	NO_3^- ($\mu\text{mol L}^{-1}$)	PO_4^{3-} ($\mu\text{mol L}^{-1}$)	Si ($\mu\text{mol L}^{-1}$)	Fe (nmol L^{-1})	Chl <i>a</i> ($\mu\text{g L}^{-1}$)	Measured ambient light	Simulated ambient light	Elevated light	In/Outdoors
NH1	60	0.7	0.5	2.3	0.27±0.08	0.55	1.2	1.5	4.5	Out
RR1	45	3.0	0.5	2.4	0.11±0.02	0.92	0.5	0.6	4.5	In
RR2	50	1.2	0.4	2.6	0.11±0.01	0.35	0.8	0.6	4.5	In
KN1	78	4.1	0.5	5.2	0.21±0.02	0.68	0.7	0.5	3.3	In
RR3	65	6.3	0.8	4.8	0.18±0.04	0.43	0.6	0.5	4.5	In
RR4	50	4.9	0.5	3.6	0.12±0.02	0.38	0.9	0.6	5.9	Out
KN2	77	1.7	0.2	2.7	0.32±0.01	0.34	0.9	1.4	4.4	In

setup from an acidic $100 \mu\text{mol L}^{-1}$ FeCl_3 stock solution. Ambient light levels at the depth of water collection were determined from photosynthetically active radiation (PAR) profiles collected on CTD casts immediately prior to GO-Flo casts for incubation setup. To set light levels for on-deck incubations (NH1, RR4), PAR measurements at depth were converted to percent surface irradiance, and an incubator was shaded with neutral-density screening to match this level with the aid of a Biospherical QSL-100 light meter. The lack of spectral correction in these outdoor incubations could have potentially affected phytoplankton growth and community structure (Wood et al. 1998). Maximum noon-time irradiances for these treatments were $15\text{--}30 \mu\text{mol photons m}^{-2} \text{s}^{-1}$. A separate incubator was shaded at 3–10-fold higher light levels, with maximum noon-time irradiances of $110\text{--}130 \mu\text{mol photons m}^{-2} \text{s}^{-1}$, for increased light treatments. For indoor incubations, the top level of the incubator, closest to the fluorescent lights, was used for high-light treatments, and the lower level was used to mimic ambient light levels at depth. Blue stage gels were used for shading, to achieve desired light intensities and approximate the spectral distribution of light at depth. The light intensities in the lower level of the incubator were set to $\sim 75\%$ of the maximal noon-time irradiance experienced at depth ($12\text{--}30 \mu\text{mol photons m}^{-2} \text{s}^{-1}$), while the upper level was set 3–9-fold higher, at $75\text{--}100 \mu\text{mol photons m}^{-2} \text{s}^{-1}$. Lights were set to turn on and off at sunrise and sunset, with a half-hour period just after sunrise and prior to sunset in which only half of the lights were on. Details of light intensities for each experiment are given in Table 1.

Chlorophyll a—Approximately 100 mL of water was gently filtered onto a GF/F filter and extracted for 24 h in 90% acetone:10% water at $0\text{--}4^\circ\text{C}$. Fluorescence of the extract was measured on a Turner 10-AU fluorometer (10-037R filter set) before and after acidification to determine chlorophyll *a* (Chl *a*) (Strickland and Parsons 1972). Eight-micrometer polycarbonate filters were used to determine size-fractionated Chl *a* ($>8 \mu\text{m}$ Chl *a*). Chl *a* was used to track phytoplankton growth in the experiments, and net Chl *a* growth rates were determined by linear regression through natural log-transformed Chl *a* data from the period of active growth (at least three time points) in each experiment. These growth rates included only increases in excess of grazing rates, which were not assessed, and the relationship between intrinsic and net growth rates in the experiments is unknown.

Nutrients—Unfiltered water samples were collected in sterile centrifuge tubes and frozen for later analysis of macronutrients to determine the course of their drawdown during incubations. Macronutrients (NO_3^- , NO_2^- , PO_4^{3-} , and Si) were determined using standard colorimetric methods by the Ocean Data Facility at Scripps Institution of Oceanography, or the Marine Science Institute Analytical Laboratory at the University of California–Santa Barbara.

Dissolved iron—For iron measurements, water from the GO-Flo bottles used to set up incubations was filtered

through an in-line $0.4\text{-}\mu\text{m}$ filter and stored acidified ($\text{pH} = 1.8$) until analysis. Iron concentrations from incubations NH1, RR1, RR3, and RR4 were measured by cathodic stripping voltammetry using the 2-(2-thiazolylazo)-*p*-cresol (TAC) ligand method described by Croot and Johansson (2000). Cleaned 4-(2-hydroxyethyl)-1-piperazinepropane-sulfuric acid (EPPS) buffer was added to water samples to a final concentration of 10 mmol L^{-1} , and the pH of the solution was brought to 8.0 using isothermally distilled ammonia. $10 \mu\text{mol L}^{-1}$ TAC was then added and the sample was analyzed on a Metrohm VA663 mercury electrode interfaced to an EcoChemie Autolab PGSTAT30 using a linear-sweep waveform. Iron was quantified by four standard additions to each sample.

For incubations RR2, KN1, and KN2, iron concentrations were measured with a chemiluminescence-detection flow-injection analysis system (Bowie et al. 1998; King and Barbeau 2007). Sulfite ($2 \mu\text{mol L}^{-1}$) was used to reduce all iron in the seawater samples to iron(II), which was then concentrated on a nitriloacetic acid resin column. Iron(II) was eluted from the column with an HCl carrier solution (0.14 mol L^{-1}) and mixed with a basic luminol-ammonia solution to initiate the chemiluminescent reaction for quantification of iron. We verified the accuracy of our implementations of the TAC electrochemical method and the chemiluminescence method through analysis of the Sampling and Analysis of iron (SAFe) iron standards. Details of SAFe standard analyses and additional information on these methods are available in Hopkinson and Barbeau (2007) and King and Barbeau (2007).

Particulate organic carbon and particulate organic nitrogen—Particulate organic carbon (POC) and particulate organic nitrogen (PON) were determined by combustion analysis. Water samples were filtered onto precombusted (450°C for 4 h) GF/F filters and stored in liquid nitrogen. Samples were exposed to fuming HCl overnight to remove inorganic carbon, dried overnight in an oven at 60°C , and subsequently analyzed on a Costech 4010 elemental combustion system at the Scripps Institution of Oceanography Analytical Facility.

Pulse amplitude-modulated (PAM) fluorometry—Phytoplankton variable fluorescence measurements to assess the quantum yield of photosystem II (PSII) were made using a Walz Xe-PAM fluorometer (Schreiber et al. 1995). Phytoplankton were acclimated to the dark for ~ 30 min prior to measurement. Probe flashes (2 Hz) from a Xenon lamp were passed through a blue filter (Schott BG39) and further attenuated with a 10% “attenuator” diaphragm plate. To saturate photosystem components, 700-ms pulses of actinic light ($>3,000 \mu\text{mol quanta m}^{-2} \text{s}^{-1}$) were supplied by a halogen lamp at 30-s intervals to allow reoxidation of reaction centers and the plastiquinone pool between pulses. Emitted chlorophyll fluorescence was passed through long-pass (RG645) and dichroic (R65) filters and measured with a photodiode detector. The described instrument configuration was checked periodically throughout cruises to ensure that Xenon flashes were not strongly actinic, and that saturating pulses allowed maximal fluorescence emission to

be reached. Initial fluorescence levels (F_0), obtained from the probe flashes alone, and maximal fluorescence (F_m), measured during application of the saturating pulses, were used to calculate $F_v:F_m$ as $(F_m - F_0)/F_m$.

High-performance liquid chromatography pigment analysis—Taxonomically informative phytoplankton pigments were analyzed by high-performance liquid chromatography (HPLC) using a modified version of the method described in Goericke and Montoya (1998). Water samples (~1 liter) were gently filtered onto GF/F filters and stored in liquid nitrogen until analysis. Filters were extracted on ice in 1.5 mL of acetone for 0.5 h, homogenized, and allowed to extract for a further 0.5 h. Following centrifugation, portions of the extract were mixed with water to produce a 60:40 acetone:water solution and immediately injected in the HPLC system. Pigments were separated on a 10-cm Alltech Adsorbosphere C8 column, using a gradient between methanol:0.5 mol L⁻¹ aqueous ammonium acetate (75:25) and methanol. Chromatographic peaks were identified by retention time and quantified by peak area using calibrations determined from pure pigments isolated from algal cultures. This method allows separation of Chl *a* and divinyl Chl *a*, and most of the abundant carotenoids. Lutein and zeaxanthin coelute with this method, but the fraction is referred to as zeaxanthin, since it is generally most abundant in oceanic samples.

Phytoplankton cell counts—Microscopic examination of phytoplankton communities from the experiments was conducted to determine the taxa and size of phytoplankton responding to treatments. Fifty-milliliter samples were preserved with ~1 mL of sodium borate-buffered formalin, concentrated in an Utermohl settling chamber, and counted on an inverted microscope using an ocular micrometer to measure cell sizes. Phytoplankton were classified based on Tomas (1997) into broad, but clearly identifiable groups. At least 100 cells in each group were counted in a sample. The most abundant groups identified were species of *Pseudonitzschia*, *Nitzschia*, and *Chaetoceros*, as well as coccolithophores and a miscellaneous class of small pennate diatoms.

Phytoplankton community structure—Pigment signatures and microscopic cell counts were used to assess phytoplankton community structure in incubation experiments. Good agreement was found between the methods where comparisons were possible, providing confidence in their utility as indicators of phytoplankton community structure. While fucoxanthin was present in a number of phytoplankton taxa, a strong correlation between fucoxanthin ($r^2 = 0.89$, $p < 0.0001$, $n = 59$) and diatom cell numbers shows that diatoms were the major contributors to fucoxanthin concentrations in the experiments. Similarly, a strong correlation between coccolithophore numbers and 19-hexanoyloxyfucoxanthin (19-hex) ($r^2 = 0.81$, $p < 0.0001$, $n = 57$) indicated that coccolithophores were the predominate contributors to 19-hex concentrations. Rarely, coccolithophores have been reported to produce 19-butanoyloxyfucoxanthin (19-but) (Jeffrey and Wright 1994), but we found only a weak

relationship between 19-but and coccolithophore numbers ($r^2 = 0.22$, $p < 0.001$, $n = 57$). Dominant contributors of 19-but are often *Phaeocystis* sp. or pelagophytes (Jeffrey and Wright 1994; Anderson et al. 1996), and while a few *Phaeocystis* colonies were observed in RR1, they were absent from other samples. Thus, 19-but was tentatively attributed to pelagophytes. Because cyanobacteria are not enumerable by the microscopic method that we used, no comparisons can be made with pigment data. However, divinyl Chl *a* (dvChl *a*) can be unambiguously attributed to *Prochlorococcus*.

Statistics—Statistical analyses were conducted on experimental results using JMP 5.1 statistical software (SAS Institute) using tests appropriate for the questions addressed. The effect of each treatment on Chl *a* growth rate, nitrate drawdown, POC content, $F_v:F_m$, and % >8 μm Chl *a* was assessed using one-way analysis of variance (ANOVA) and post-hoc Tukey–Kramer tests. Although these tests assume equal variance among treatments, it was clear that variance was generally lower in ambient light treatments where less growth occurred. Consequently, selected data from the ambient light treatments were retested without high-light data using one-way ANOVA as noted. To determine whether there was a significant interaction between iron and light, two-way ANOVA analyses with light and iron as independent factors were conducted. To assess the effect of iron on Chl *a* and fucoxanthin concentrations at each light level, Student's *t*-tests were employed. Despite the low replication of each treatment ($n = 2$), statistical significance ($p < 0.05$) in the experimental results was generally found.

Results

In this first attempt to study iron–light colimitation at SCMs, we sought to assay a variety of regions, ranging from mesotrophic to oligotrophic. All experiments showed some characteristic responses of growth rate, changes in phytoplankton community structure, and changes in physiology to iron addition. In some experiments, phytoplankton responses to iron were observed at ambient light levels, and in these experiments, strong, immediate responses to iron at elevated light were also observed (experiments NH1, RR1, RR2, KN1; Table 2). In other experiments, no responses were observed at ambient light, but responses to iron were observed in elevated light treatments after some nutrient drawdown had occurred (experiments RR3, RR4, KN2; Table 2). The differential responses were likely a consequence of variable initial conditions and stresses between and within the sampled SCMs, which potentially depend on factors that are difficult to constrain, such as the history of each feature. However, when observed, responses of phytoplankton physiology and community structure to iron addition were generally similar throughout the experiments; this is discussed in more detail in the following sections.

Initial conditions—Iron and light manipulation experiments were conducted at SCMs in mesotrophic to

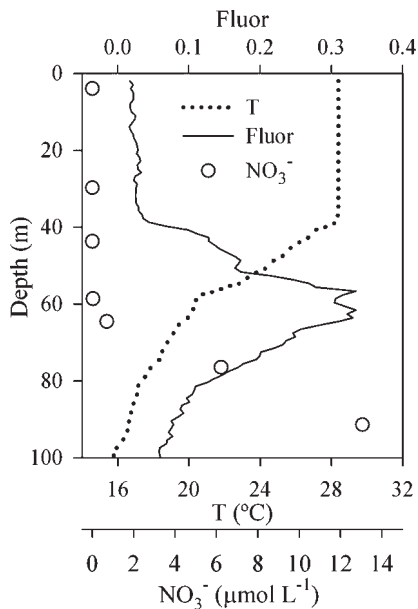


Fig. 4. Profiles of Chl *a* fluorescence (Fluor, relative units), temperature (T), and nitrate (NO_3^-) at a station ($17^\circ 24' \text{N}$, $108^\circ 17' \text{W}$) in the eastern tropical North Pacific where NH1 was initiated. SCM and water-column structure at this station are typical of the stations sampled in this study. Water for NH1 was collected at 65-m depth, within the subsurface chlorophyll maximum, and at the top of the nitracline.

oligotrophic waters of the SCB and ETNP. In the SCB, where oceanic domains have been better defined, RR1 and RR3 were conducted within the coastal domain, while all other incubations were collected from offshore sites (Fig. 3; Hayward and Venrick 1998). All SCMs sampled in this study were also biomass maxima, as indicated by transmissometer data (data not shown), as opposed to purely Chl *a* maxima produced by photoacclimation, which are often found in oligotrophic gyres (Cullen 1982). Water for experiments was collected from within the SCM, near the top of the nitracline, and the range of initial Chl *a* was $0.34\text{--}0.92 \mu\text{g L}^{-1}$, NO_3^- was $0.7\text{--}6.3 \mu\text{mol L}^{-1}$, dissolved Fe was $0.11\text{--}0.32 \text{ nmol L}^{-1}$, and ambient light levels were $0.5\text{--}1.2\%$ surface irradiance (Table 1). A representative water-column profile from the station where NH1 was initiated is shown in Fig. 4. This profile demonstrates the relationship between the nitracline and SCM common to all sites in this study, and it shows the approximate gradient of the nitracline at our study sites. Although the nitracline is relatively steep, we were successful in capturing the top of it in most incubations (Table 1). For stations where data are available, surface mixed-layer iron concentrations were slightly lower than SCM concentrations, indicating that water for incubations was collected near the top of the ferricline (surface dissolved iron for NH1: $0.11 \pm 0.02 \text{ nmol L}^{-1}$; KN1: $0.13 \pm 0.01 \text{ nmol L}^{-1}$; KN2: $0.22 \pm 0.01 \text{ nmol L}^{-1}$). However, because data are available for only three stations, it is difficult to generalize. With the exception of KN1, phytoplankton communities were typical of those commonly found in the study regions (Venrick 1998, 2000). At the KN1 site, phytoplankton species at the SCM were

typical of offshore communities but were present at elevated abundances relative to historical data (see Discussion).

Chl *a*: Concentrations and growth rates—One incubation experiment from the ETNP (NH1) and two from the SCB (RR2, KN1) showed increases in Chl *a* concentrations and Chl *a*-derived growth rates in response to increased iron and both ambient and elevated light levels. In these experiments, +Fe and +L treatments resulted in moderate increases in Chl *a* concentrations, but a strong, synergistic effect of increased iron and light (+Fe+L) led to dramatic increases in Chl *a* and net phytoplankton growth rates (Fig. 5A; Tables 2, 3). Separation of iron-addition treatments from their respective controls (C, +L) occurred immediately after growth began. In RR1, an immediate response to iron was seen at elevated light levels, and although at ambient light, no significant Chl *a* response to iron was seen, responses to iron were observed in other parameters (Tables 2, 3; see below). In the remainder of the incubations (RR3, RR4, KN2), no differences between ambient light treatments were observed in Chl *a* concentrations or growth rates, but at elevated light, Chl *a* growth in +Fe+L treatments eventually outpaced +L treatments, after an initial period in which the treatments tracked each other (Fig. 5B; Tables 2, 3). Interpretation of Chl *a* results as a proxy for phytoplankton biomass and growth rate is complicated by differences in phytoplankton carbon (C):Chl *a* ratios between treatments. As indicated by POC:Chl *a* (g:g) ratios within our experiments (+Fe+L: $44\text{--}51$; +L: $77\text{--}123$), iron stress generally increases C:Chl *a*, as does higher light intensity (Geider et al. 1998). Additionally, because Chl *a* is a community parameter, calculated net community growth rates reflect both growth in response to treatments and loss by grazing or cell death, particularly of cyanobacteria (see below), which may lead to an early drop in Chl *a* in some incubations and lowers net growth rates in these experiments (Fig. 5A).

Nutrient drawdown—The macronutrients NO_3^- , NO_2^- , PO_4^{3-} , and Si were measured daily in each incubation, but the results presented will focus on NO_3^- , since it was depleted first in incubations where complete nutrient drawdown was reached. At elevated light, nitrate drawdown generally followed Chl *a* increases, and faster rates of drawdown occurred in +Fe+L treatments immediately (NH1, RR1, RR2, KN1; Fig. 5C) upon, or after, the occurrence of some nutrient drawdown, and responses to iron were observed in Chl *a* (RR3, RR4, KN2; Fig. 5D). Nearly complete drawdown of nitrate was observed in many +Fe+L treatments, at which point incubations were harvested to avoid “crashing” of incubations (when nutrient exhaustion leads to phytoplankton senescence). Although diatoms came to dominate +Fe+L treatments (see below), Si was only exhausted in RR1 concomitantly with nitrate, and it remained at concentrations $>1 \mu\text{mol L}^{-1}$ in all other experiments (data not shown). $\text{NO}_3^-:\text{PO}_4^{3-}$ drawdown ratios approximated Redfield ratios and were not different between treatments (+Fe+L: 15 ± 4 ; +L: 15 ± 3). Si: NO_3^- drawdown ratios varied widely among

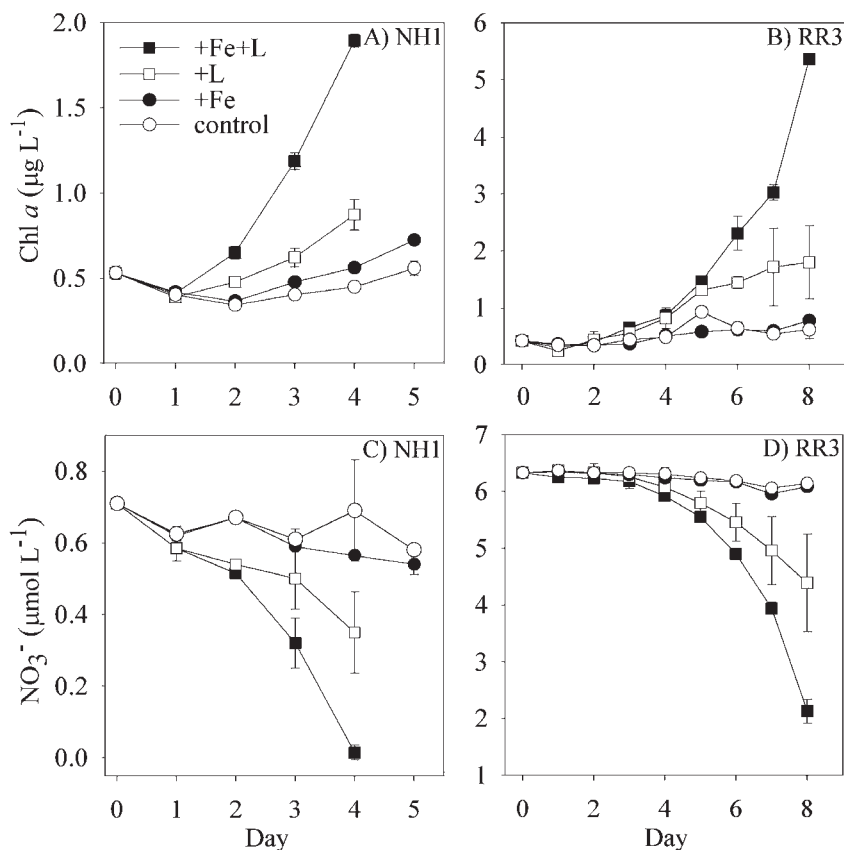


Fig. 5. (A, B) Chl *a* and (C, D) nitrate data from incubations NH1 (panels A, C) and RR3 (panels B, D), which are representative of the two general classes of observed responses to iron at ambient and elevated light (NH1), and delayed responses to iron only at elevated light (RR3). Error bars represent the standard deviation between replicate bottles and, when not visible, are smaller than the symbols.

experiments and treatments, reflecting primarily the abundance of diatoms in each sample, as opposed to the effects of iron on silicification, which have been documented (data not shown; Hutchins et al. 1998). In ambient light treatments, changes in nitrate were generally small but measurable (Table 2), though changes in other macronutrients were not resolved (data not shown). No significant differences between treatments were seen.

POC and PON—Initial POC data from several incubations (RR2: 3.4 μmol L⁻¹; KN1: 7.6 μmol L⁻¹) showed that only small increases occurred in +Fe and control treatments, but significant growth occurred in elevated light treatments (Table 2). At ambient light, significantly higher POC concentrations were only observed in +Fe treatments of incubations KN1 and RR4, although, because no other responses to iron were observed at ambient light for RR4, this measurement was apparently an anomaly. At elevated light, POC concentrations in +Fe+L treatments were approximately double those of +L treatments, except for RR2, where POC concentrations were similar in both treatments. These observations are consistent with nitrate drawdown in each incubation. In RR1 and RR2, ratios of POC increase to PON increase in +Fe+L treatments (RR1: 12.5; RR2: 10.5) were higher than

+L treatments (RR1: 8.4; RR2: 7.0), and they were in excess of expected Redfield ratios (6.6). In other incubations, no differences were seen between +Fe+L and +L treatments, and ratios were closer to Redfield values (+Fe+L: 7.2 ± 0.4; +L: 7.3 ± 1.2). The previous calculations assume that initial POC values were similar to final control treatment concentrations since initial POC data are lacking for most incubations, but similar trends are observed in final POC: PON ratios despite the possible complications from detrital material (RR1 +Fe+L: 9.9, +L: 7.2; RR2 +Fe+L: 8.6, +L: 6.6).

$F_v : F_m$ —PAM fluorometric measurements of $F_v : F_m$, the maximum efficiency of light utilization in PSII, were collected daily for all incubations except NH1 (Fig. 6; Table 4). At ambient light, $F_v : F_m$ remained constant or increased moderately in controls and had significantly higher values in +Fe treatments in RR2 and KN1, indicating that higher iron availability led to an increase in photosynthetic efficiency in these incubations, where responses to iron were observed in other parameters at ambient light (Fig. 6A; Table 4). In RR1, $F_v : F_m$ was also elevated in +Fe treatments compared with controls, though the result was not statistically significant. In experiments RR3, RR4, and KN2, no differences in $F_v : F_m$ were

Table 2. Incubation responses to iron and light manipulations. Growth rates derived from Chl *a* (μ_{Chl}), drawdown in nitrate over the course of the experiment (ΔNO_3^-), and particulate organic carbon (POC) concentrations for each treatment are given as the mean of replicate bottles, and the standard deviation between replicates is reported in parentheses below. Each experiment was analyzed with one-way ANOVA and post-hoc Tukey–Kramer tests to determine significant ($p < 0.05$) differences between treatment means. Values with significantly different means are marked with a different letter. A two-way ANOVA was run on each experiment to determine whether there was a significant ($p < 0.05$) interaction term between the independent factors of iron and light. Experiments in which significant interaction terms were found are marked with an asterisk (*) next to the +Fe+L value. Finally, because variances were lower in ambient light treatments, a *t*-test was performed only on control and +Fe data, and significant ($p < 0.05$) differences between these treatments are indicated with a “t” next to the +Fe value. For incubations NH1 and KN2, POC data are not available, as indicated by n.d. (no data).

	Ambient- and high-light iron responses				High-light iron response		
	NH1	RR1	RR2	KN1	RR3	RR4	KN2
μ_{Chl} (d^{-1})							
control	0.16 ^A (0.01)	0.00 ^A (0.04)	0.08 ^A (0.01)	0.01 ^A (0.00)	0.08 ^A (0.04)	0.02 ^A (0.01)	0.17 ^A (0.04)
+Fe	0.22 ^{A,B,t} (0.01)	0.03 ^A (0.08)	0.13 ^A (0.03)	0.05 ^{A,t} (0.02)	0.12 ^A (0.02)	0.03 ^A (0.04)	0.16 ^A (0.00)
+L	0.30 ^B (0.04)	0.28 ^B (0.03)	0.15 ^A (0.02)	0.19 ^B (0.00)	0.25 ^{A,B} (0.12)	0.16 ^B (0.01)	0.39 ^B (0.03)
+Fe+L	0.53 ^{C,*} (0.04)	0.60 ^{C,*} (0.00)	0.27 ^B (0.01)	0.49 ^{C,*} (0.03)	0.42 ^B (0.01)	0.32 ^{C,*} (0.04)	0.70 ^{C,*} (0.04)
ΔNO_3^- ($\mu\text{mol L}^{-1}$)							
control	0.13 ^A (0.01)	0.11 ^A (0.05)	0.15 ^A (0.02)	0.67 ^A (0.06)	0.28 ^A (0.02)	0.13 ^A (0.10)	0.22 ^A (0.06)
+Fe	0.17 ^A (0.03)	0.13 ^A (0.23)	0.14 ^A (0.02)	0.82 ^A (0.07)	0.30 ^A (0.01)	0.05 ^A (0.09)	0.28 ^A (0.00)
+L	0.36 ^B (0.11)	1.85 ^B (0.10)	0.82 ^B (0.07)	1.58 ^B (0.17)	1.95 ^B (0.86)	0.85 ^B (0.36)	1.42 ^B (0.08)
+Fe+L	0.70 ^{C,*} (0.02)	3.00 ^{C,*} (0.01)	0.99 ^{C,*} (0.02)	3.74 ^{C,*} (0.32)	4.20 ^{C,*} (0.21)	1.22 ^{C,*} (0.16)	1.54 ^B (0.00)
POC ($\mu\text{mol L}^{-1}$)							
control	n.d.	9.0 ^A (1.3)	5.2 ^A (0.1)	9.2 ^A (0.1)	5.4 ^A (0.4)	3.1 ^A (0.1)	n.d.
+Fe	n.d.	9.5 ^A (3.3)	4.9 ^A (0.4)	10.0 ^{A,B,t} (0.2)	5.0 ^A (0.8)	4.5 ^{B,t} (0.3)	n.d.
+L	n.d.	21.7 ^B (0.8)	12.0 ^B (0.1)	12.7 ^B (0.3)	13.1 ^B (1.8)	6.5 ^C (0.3)	n.d.
+Fe+L	n.d.	37.1 ^{C,*} (3.7)	13.7 ^{C,*} (0.1)	24.5 ^{C,*} (1.4)	23.1 ^{C,*} (2.7)	10.0 ^{D,*} (0.7)	n.d.

observed between control and +Fe treatments (Fig. 6B; Table 4). When light was elevated, $F_v:F_m$ declined relative to initial values in +L treatments in all experiments for which data were available, but values remained constant or increased slightly in +Fe+L treatments. In incubations where immediate declines in $F_v:F_m$ were observed in +L treatments, a portion of this response may have been due to photoinhibition, but the continued decline of $F_v:F_m$ in +L treatments as growth proceeded was likely caused by increasing iron stress as available iron was consumed (Fig. 6A). In other experiments, the drops were coincident with separation between +L and +Fe+L treatments in several variables, indicating that Fe stress was the major factor reducing $F_v:F_m$ (Fig. 6B). Although nitrate concentrations were low at the start of some experiments, and

nearly exhausted in many +Fe+L treatments, no dramatic declines in $F_v:F_m$ were observed in the +Fe+L treatments, suggesting that nitrogen availability did not have a major effect on photosynthetic efficiency in the experiments (Fig. 6).

Phytoplankton community structure—Pigment data showed that the initial SCM phytoplankton communities were relatively diverse; significant amounts of fucoxanthin (diatoms), 19-hexanoyloxyfucoxanthin (19-hex, prymnesiophytes), 19-butanoyloxyfucoxanthin (19-but, pelagophytes), and divinyl Chl *a* (dvChl *a*, *Prochlorococcus* sp.) were present and attributable to distinct phytoplankton taxa (Fig. 7). At ambient light levels, only fucoxanthin increased in response to iron additions in those incubations

Table 3. Effect of iron addition on pigments at each light level. Data are reported as ratios of pigments ($\mu\text{g L}^{-1}:\mu\text{g L}^{-1}$) to facilitate intercomparison, and standard deviations are reported in parentheses below. Significant differences ($p < 0.05$) between treatments (+Fe vs. control or +Fe+L vs. +L) are indicated by an asterisk (*), as determined using a one-way ANOVA on the pigment concentrations in each treatment.

	Ambient- and high-light iron responses				High-light iron response		
	NH1	RR1	RR2	KN1	RR3	RR4	KN2
Chl <i>a</i> +Fe/C	1.29*	1.31	1.26*	1.32*	1.05	1.29	1.23
	(0.10)	(0.62)	(0.09)	(0.17)	(0.15)	(0.29)	(0.20)
Chl <i>a</i> +Fe+L/+L	2.2*	2.8*	1.5*	5.5*	3.0*	2.8*	1.6*
	(0.2)	(0.4)	(0.2)	(1.1)	(1.0)	(0.2)	(0.1)
Fucox+Fe/C	1.43*	1.40	1.38	1.68*	1.08	0.92	0.88
	(0.11)	(0.33)	(0.30)	(0.10)	(0.08)	(0.26)	(0.04)
Fucox+Fe+L/+L	2.16*	1.58*	1.39*	5.82*	3.72*	3.08*	1.95*
	(0.17)	(0.03)	(0.03)	(0.09)	(1.04)	(0.20)	(0.20)

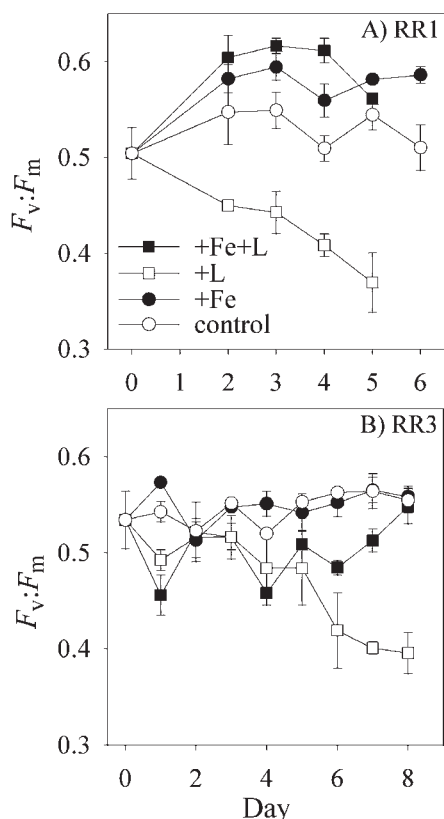


Fig. 6. Increases in $F_v:F_m$ relative to control and +L treatments were seen in +Fe and +Fe+L treatments in (A) RR1, while in (B) RR3, declines in +L treatments were seen after separation between +Fe+L and +L treatments occurred in other parameters (Fig. 5B,D). Error bars represent the standard deviation between replicate bottles.

where Chl *a* responses were also observed (Table 3; Fig. 7A). In other experiments, no differences in pigment concentrations were seen at ambient light (Table 3; Fig. 7C). In all incubations, significantly higher levels of fucoxanthin were found in +Fe+L compared to +L treatments when incubations were terminated (Table 3; Fig. 7A,C). While many taxa other than diatoms contain

fucoxanthin, including prymnesiophytes and pelagophytes, they typically have additional accessory carotenoids, such as 19-hex or 19-but. In all cases except one (KN1), these pigments did not respond significantly to iron in our experiments, suggesting that diatoms were the primary taxon affected by iron limitation. Other pigments (19-hex, 19-but) increased in +L and +Fe+L treatments over +Fe and C treatments but showed no differences between iron treatments, indicating that the net growth rate of phytoplankton containing these pigments was light-limited in most incubations (Fig. 7A,C). Significant responses to iron were observed in other pigments only in KN1 (Fig. 8B). In this incubation, 19-hex was slightly elevated in +Fe relative to control treatments, and both 19-hex and 19-but were elevated in +Fe+L treatments compared to +L treatments, showing that iron has the potential to affect members of the phytoplankton community other than diatoms.

The behavior of cyanobacterial pigments (dvChl *a*, zeaxanthin) varied among our experiments, though no responses to iron were observed (data not shown). At ambient light levels, cyanobacterial pigments were approximately constant in most incubations; however, declines were observed in NH1 and KN1. In RR4, increases in dvChl *a* were observed at elevated light, but in many cases (NH1, RR3, RR2, KN1), elevated light levels led to declines in cyanobacterial pigments. The cause, whether it was due to photoacclimation or growth inhibition, is unknown. As indicated by pigment signatures, the most prominent change in community structure was a shift to diatom dominance when light and iron availability increased.

Microscopic analysis of preserved phytoplankton generally confirmed changes in diatom and coccolithophore abundances inferred from pigment data, although some discrepancies were noted, most likely due to changes in cellular pigment contents of phytoplankton between treatments. Diatoms were initially present at low numbers in all incubations except RR1, where *Chaetoceros* were abundant (data not shown; see also Fig. 10A). At elevated light, diatom abundances, especially *Pseudonitzschia* and *Nitzschia*, increased and responded to iron—cell numbers in +Fe+L treatments were roughly double those in +L

Table 4. $F_v:F_m$ at the final time point of incubations, except NH1, where variable fluorescence data were not collected. Data are averages and standard deviations (in parentheses) between replicate bottles. Each experiment was analyzed with one-way ANOVA and post-hoc Tukey–Kramer tests to determine significant ($p < 0.05$) differences between treatment means. Values with significantly different means are labeled with different letters.

	RR1	RR2	KN1	RR3	RR4	KN2
Initial	0.50 ^A (0.03)	0.48 ^A (0.02)	0.60 ^A (0.00)	0.53 ^A (0.03)	0.51 ^A (0.04)	0.61 ^{A,B} (0.01)
Control	0.51 ^A (0.02)	0.54 ^B (0.01)	0.60 ^A (0.01)	0.55 ^A (0.01)	0.59 ^B (0.01)	0.61 ^A (0.04)
+Fe	0.59 ^A (0.01)	0.60 ^C (0.01)	0.64 ^B (0.01)	0.56 ^A (0.01)	0.63 ^{A,B} (0.01)	0.63 ^A (0.00)
+L	0.37 ^B (0.03)	0.40 ^D (0.00)	0.52 ^C (0.01)	0.39 ^B (0.02)	0.43 ^C (0.01)	0.50 ^B (0.01)
+Fe+L	0.56 ^A (0.01)	0.56 ^{A,B} (0.01)	0.66 ^B (0.01)	0.55 ^A (0.02)	0.56 ^{A,B} (0.01)	0.59 ^A (0.01)

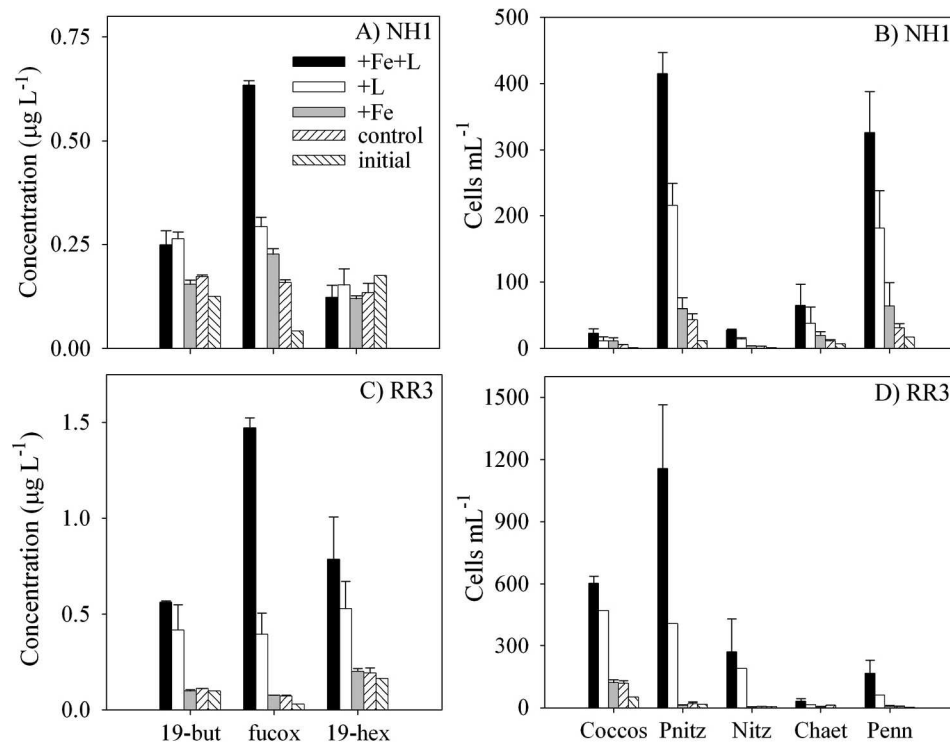


Fig. 7. Responses of phytoplankton taxa to iron and light manipulations in (A, B) NH1 and (C, D) RR3. Differential responses were observed in the most abundant pigments (panels A, C) 19-butanoyloxyfucoxanthin (19-but), which responded only to light, fucoxanthin (fucox), which responded to iron and light, and 19-hexanoyloxyfucoxanthin (19-hex), which remained constant in NH1 and responded to light in RR3. Microscopic analysis (panels B, D) confirmed that diatoms dominated the response to increased iron and light. Enumerated phytoplankton were grouped into broad classes, the most abundant of which are graphed: Coccolithophores (Coccus), *Pseudonitzschia* species (Pnitz), *Nitzschia* species (Nitz), *Chaetoceros* species (Chaet), and miscellaneous small pennates (Penn). Error bars represent the standard deviation between replicate bottles.

treatments, which is consistent with POC increases and nitrate drawdown (Fig. 7B,D). C and +Fe treatments also had more diatoms relative to initial conditions, and there were often more diatoms in +Fe treatments, though the difference was not statistically significant in any experiment (Fig. 7B). The diatoms were large compared to the majority of the phytoplankton community; *Pseudonitzschia* individuals measured between 20 μm and 100 μm in length, *Nitzschia* individuals were 25–180 μm , miscellaneous small pennates were 6–20 μm , and *Chaetoceros* individuals were 5–25 μm . Coccolithophores also increased at elevated light and were moderately higher in some +Fe+L treatments compared to +L treatments, although the differences were not statistically significant in any experiment, suggesting that at least some of the increase of 19-hex in +Fe+L treatments of KN1 was due to increased pigment per cell (Fig. 8B). Increases of coccolithophores at ambient light were observed relative to initial conditions, but no responses to iron were seen (Fig. 7B,D).

Size-fractionated (>8 μm) Chl *a* from the RR experiments showed initial phytoplankton were mostly smaller than 8 μm (Table 5), except for RR1, which was taken from a more productive water column with higher initial Chl *a* (Table 1) and a greater proportion of phytoplankton

biomass present as larger diatoms. The proportion of Chl *a* in the >8- μm size class did not change significantly from initial conditions in ambient light treatments, except in RR1, where a decrease was observed in both +Fe and control treatments. In contrast, at elevated light, the fraction of Chl *a* >8 μm increased moderately in +L treatments and dramatically in +Fe+L treatments, consistent with microscopic observations, which showed that larger diatoms grew more rapidly when iron availability increased (Table 5).

Discussion

The results of these experiments suggest that iron availability is an important factor modulating phytoplankton growth rate and community structure in the SCMs studied, despite macronutrient limitation of the surface waters. Laboratory studies that suggested elevated iron requirements at low light may lead to iron–light colimitation of phytoplankton growth rates motivated our investigations and experimental design, and two general classes of responses to experimental manipulation of iron and light were observed. In four incubations (NH1, RR1, RR2, and KN1), responses to iron addition were observed at both

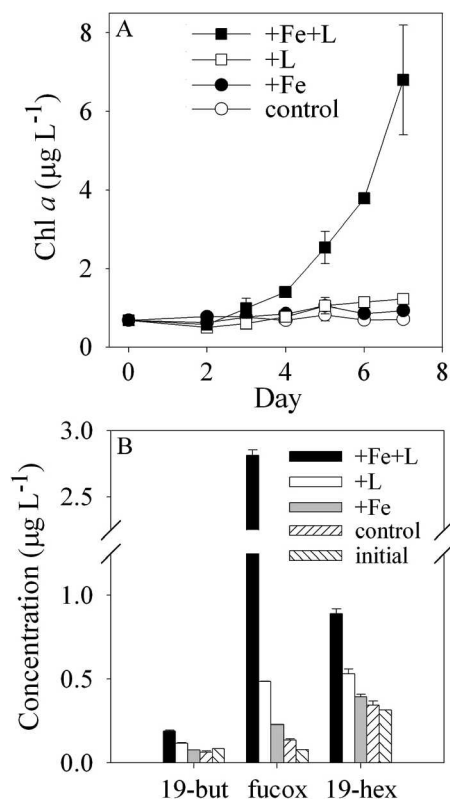


Fig. 8. Responses suggestive of iron–light colimitation of the eukaryotic phytoplankton community were observed in incubation KN1, which was initiated from an anomalously strong subsurface chlorophyll maximum believed to be the result of a nutrient input event (*see* Discussion). (A) Statistically significant Chl *a* increases were observed in +Fe and +L treatments relative to controls (Table 3). (B) Taxonomic pigments showed that diatoms (fucox), prymnesiophytes (19-hex), and pelagophytes (19-but) all showed responses characteristic of iron–light colimitation, in contrast to other experiments. Error bars represent the standard deviation between replicate bottles.

ambient and elevated light, a combination indicative of iron–light colimitation within these SCMs (Tables 2, 3). In other experiments (RR3, RR4, and KN2), iron had no observable effect on phytoplankton at ambient light, but at elevated light, iron addition resulted in faster growth and higher phytoplankton biomass after some nutrient draw-down had occurred. These results indicate that light was the proximate limiting factor at the stratum sampled, but the community could readily be driven into iron limitation upon relief of light limitation. Based on these findings, iron availability may become important when SCM light levels are elevated rapidly and decoupled from supplementary iron inputs, as can occur in upwelling eddies or strong internal waves.

Iron–light colimitation—In traditional concepts of growth limitation, only one nutrient, the least available, is relevant to understanding constraints on growth rate. More thorough knowledge of autotrophic physiology has revealed that numerous links among nutrients exist, involving acquisition and elemental substitution, which complicate

Table 5. Size-fractionated Chl *a* in select incubations. Values are the mean from replicate bottles, and standard deviations between bottles are reported in parentheses below. Each experiment was analyzed with one-way ANOVA and post-hoc Tukey–Kramer tests to determine significant ($p < 0.05$) differences between treatment means. Values with significantly different means are marked with different letters. For some initial measurements, only one sample was taken, and so no standard deviations are available (n.d.), and these data were not included in the ANOVA analysis.

% Chl <i>a</i> >8 μm	RR1	RR2	RR3	RR4
Initial	65 ^A (5)	6 (n.d.)	9 (n.d.)	21 ^A (2)
control	26 ^B (4)	7 ^A (1)	12 ^A (0)	29 ^{A,B} (18)
+Fe	25 ^B (17)	9 ^A (1)	14 ^A (2)	45 ^{B,C} (1)
+L	67 ^A (11)	9 ^A (1)	18 ^A (3)	28 ^{A,B} (5)
+Fe+L	86 ^A (1)	22 ^B (4)	34 ^B (4)	66 ^C (7)

attempts to identify a single limiting nutrient in many situations (e.g., Price and Morel 1990; Sunda and Huntsman 1997). Additionally, in the pelagic marine environment, diverse phytoplankton with different nutrient requirements are typically present and are potentially limited by different factors. Taking into account these complications, more recent considerations of nutrient limitation have recognized the existence of colimitations at the organismal and community level (Arrigo 2005; Saito et al. 2008). A cellular-level colimitation by iron and light was hypothesized by Sunda and Huntsman (1997) on the basis of the high iron requirements of photosynthetic-reaction-center and electron-transport proteins. Studies in deeply mixed HNLC waters have provided some evidence that this colimitation occurs in the field (Maldonado et al. 1999; Boyd et al. 2001). We sought to examine the possibility that iron and light colimit phytoplankton growth rate at SCMs of non-HNLC, stratified waters columns.

In several incubation experiments from the ETNP and SCB (NH1, RR1, RR2, KN1), phytoplankton community responses indicative of iron–light colimitation were observed. Increases in Chl *a*-derived growth rates were found in all elevated light treatments and were generally observed in response to added iron (Table 2). Importantly, a synergistic effect on Chl *a* growth rates was observed in response to increased iron and light. Taxonomic pigment and microscopic data showed that diatoms were generally the only taxon to respond to iron at both ambient and elevated light, suggesting that the colimitation could be occurring at a cellular level (Fig. 7). Because of biases in Chl *a* and carotenoid pigments as an indicator of phytoplankton biomass when light and iron levels are changing, the similar responses of nitrate drawdown, POC increases, and cell numbers to the treatments are notable (Fig. 5C; Table 2). The lack of significant response of POC, cell numbers, or nutrient drawdown to iron addition at ambient light in incubations NH1, RR1, and RR2 is the

primary difference between the behavior of these parameters and that of Chl *a*. Phytoplankton biomass may not have increased significantly in +Fe treatments during the course of these experiments. In these cases, it could be argued from a phenomenological perspective that colimitation of growth rate was not observed because one parameter (Fe) did not produce significant biomass and net growth rate increases on its own.

However, in the context of the hypothesized physiological basis for iron–light colimitation, additional considerations are relevant. The fact that this colimitation would operate at a cellular level complicates conclusive demonstration, since our data are at a community or multispecies taxonomic level, but several lines of evidence are consistent with colimitation due to the need for iron in photosynthetic proteins. A significant interaction effect between iron and light is observed on Chl *a* growth rates; this result would be expected under the conceptual model for iron–light colimitation, where the linked physiology of light and iron mean they would be expected to synergistically increase growth rate (Sunda and Huntsman 1997). Taxonomic pigment data and microscopic cell counts show that responses characteristic of colimitation were generally confined to diatoms. These data rule out the possibility that widely different taxa were independently responding to iron and light, and they strongly suggest that the interactive effects of iron and light were occurring at a cellular level. Increases in $F_v:F_m$ in response to iron addition at ambient and elevated light demonstrated that added iron was routed to the photosynthetic apparatus, allowing more efficient light utilization in PSII (Greene et al. 1992). While this does not rule out the possibility that iron had additional effects on phytoplankton physiology, it does show that some added iron was used in photosynthetic proteins, as would be expected in an iron–light colimited state induced by photosynthetic iron requirements. The feature of iron–light colimitation that was most problematic to demonstrate in our experiments is an increase in growth rate in +Fe treatments.

Iron clearly had an effect on the phytoplankton community at ambient light, as evidenced by increases in Chl *a*, fucoxanthin, and $F_v:F_m$, but what is the significance of these data? As discussed already, increases in $F_v:F_m$ indicate an increased efficiency of light utilization in PSII, which would potentially allow more efficient photosynthesis and higher growth rates. The most conservative interpretation of the Chl *a* and carotenoid pigment increases in +Fe treatments is that they represent higher cellular pigment contents. Changes in cellular Chl *a* and accessory pigments reflect acclimation of the photosynthetic apparatus to match light harvesting with requirements for growth (Geider et al. 1998). The increased pigments per cell in conjunction with increased $F_v:F_m$ thus suggest an improved capacity to productively harvest light. Such an adjustment is consistent with the hypothesized physiological basis for iron–light colimitation. A modest increase in diatom growth rate may have occurred but did not produce observably higher biomass for a number of reasons, such as (1) grazing kept up with relatively small increases in growth rate, or (2) since diatoms were only a

modest portion of the community, changes in bulk parameters were difficult to detect (and microscopic counts had high variability).

While there is strong evidence that diatom growth rates were iron–light colimited, it is difficult to conclusively demonstrate iron–light colimitation of growth rates from these experiments. However, the data show that there is a strong effect of iron addition at elevated light and suggest that iron is an important factor controlling growth rate and community structure at SCMs. Macronutrients are certainly also major determinants of productivity and community structure in these SCMs, particularly in their upper portions above the nitracline (Herbland and Voituriez 1979; Cullen 1982). Iron may have a significant role within the nitracline, where macronutrient limitation is relieved but light levels are low, exacerbating iron stress. Responses characteristic of iron–light colimitation were observed in waters with relatively low initial iron concentrations (0.11–0.21 nmol L⁻¹) in three of the SCMs, but the iron concentration was somewhat higher (0.27 nmol L⁻¹) in the ETNP, which may have been due to its location over a suboxic zone (Table 1; Deutsch et al. 2001; Hopkinson and Barbeau 2007). Similar behavior of phytoplankton communities in both the tropical and subtropical Pacific and in waters of varying productivity indicates that iron may be an important factor throughout SCMs in the eastern Pacific, where iron supply is generally low.

Role of iron under changing light levels—While our experiments were designed to test for iron–light colimitation and responses suggestive of this state were observed in certain SCMs, at other stations, phytoplankton responses to iron were seen only at elevated light. Lack of responses at ambient light and delayed onset of iron limitation at high light suggest that iron availability was initially higher in these experiments, and it was subsequently depleted to limiting concentrations as growth occurred. Although measured iron concentrations were no different from other experiments (Table 1), small changes in iron bioavailability not resolvable by our measurements could have supported the small amount of growth observed prior to the onset of iron stress (Fig. 5B,D), given that N:Fe ratios can reach 15,000 for iron-limited phytoplankton (Price 2005). Although a response to iron occurred only at elevated light in these experiments, the effects of iron on phytoplankton physiology and community structure were nearly identical to those observed in the other set of experiments, in which responses to iron were seen at ambient and elevated light.

Factors responsible for the different incubation responses are currently speculative since initial conditions, most notably iron and light levels, were similar. Initial parameters showed no statistically significant differences between incubations where responses characteristic of iron–light colimitation were observed and those in which only high-light responses to iron were found. However, because of the limited data set, detection of such differences may be difficult. In general, Chl *a* levels were lower and nitrate levels were higher at SCM strata where only high-light responses to iron were observed (Table 1). It is possible that these incubations were initiated from deeper within the

nitracline, where iron availability may also have been higher, since iron concentrations through the water column are generally correlated with nitrate. However, in some water columns, this relationship breaks down, and the ferricline is found deeper than the nitracline, potentially exacerbating iron stress at the SCM (Johnson et al. 1997a,b). The causes of this offset are still under investigation, but possibilities include increased uptake of iron by organisms at depth, or differential rates of remineralization of iron and nitrogen from sinking materials (Frew et al. 2006). Iron stress at SCMs may vary depending on the relationship between the ferricline and nitracline, potentially providing an alternate explanation for the different incubation responses observed.

Although we cannot fully explain the origin of the different experimental responses, in all incubations, the effects of iron addition on growth and community structure were consistent and dramatic at elevated light levels (Table 2; Fig. 7). Since iron requirements are expected to be lower at higher light levels, this finding may seem counterintuitive. However, the effects of iron and light are synergistic under the proposed physiological model for interactions between iron and light limitation, and so availability of either factor will have a proportionally greater effect when the other is replete (Fig. 1). Additionally, continued depletion of iron as growth occurs at elevated light probably contributes to the greater observed effect of iron at elevated light levels. Our results therefore indicate that iron availability may have an especially strong influence on SCMs when light levels increase due to, for example, upwelling eddies, internal waves, or changes in cloud cover (Lande and Yentsch 1988; McGillicuddy et al. 1998; Letelier et al. 2004). By lifting the nutricline further into the euphotic zone, mesoscale upwelling eddies effectively raise the local light level of nutrient-rich waters, a situation analogous to our +L treatments, indicating that iron availability could be an important control on community structure and nutrient cycling within these features. This scenario assumes that eddies act solely to dome isopycnals, preserving relationships between the ferricline and nitracline, which is their effect to a first approximation (McGillicuddy et al. 1998). However, eddy doming may also be accompanied by diapycnal mixing or vertical transport, which would complicate a simple model of their biogeochemical effect (McGillicuddy et al. 2007). Eddies are important mechanisms of nutrient supply to oligotrophic regions—accounting for about half of new production in the Sargasso Sea—but the episodic nature of mesoscale eddies complicates efforts to study them (McGillicuddy et al. 1998; Benitez-Nelson et al. 2007).

We encountered an anomalously strong subsurface chlorophyll maximum in oligotrophic waters at the edge of the North Pacific Gyre from which KN1 was initiated (Fig. 9). The phytoplankton community there was dominated by flora characteristic of the North Pacific Gyre (Venrick 2000; E. Venrick pers. comm.), which suggests that the high biomass was the result of a local nutrient input event, most likely due to isopycnal shoaling. Dramatic increases in growth rate were observed when iron and light availability were both elevated in KN1

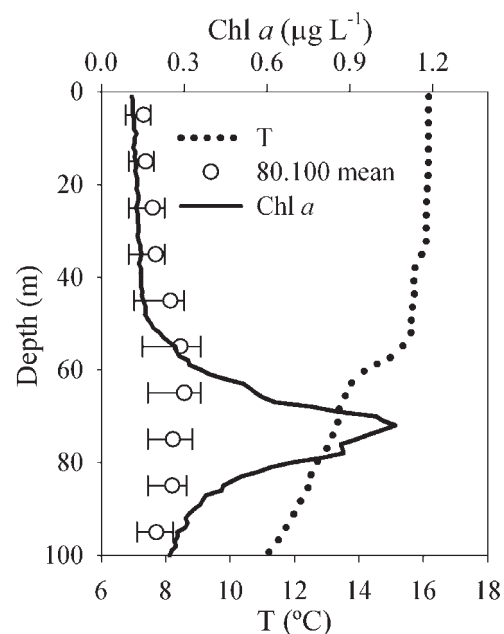


Fig. 9. An unusually strong subsurface chlorophyll maximum where KN1 was initiated. A water-column profile is shown of Chl *a* fluorescence (calibrated with discrete Chl *a* samples collected on the CTD cast) and temperature (T) at a station on the edge of the North Pacific Gyre (Fig. 2). Maximum Chl *a* concentrations of $1 \mu\text{g L}^{-1}$ are much higher than typically observed at SCM in this region. Shown for comparison are historical Chl *a* data from CalCOFI station 80.100, the closest station to where KN1 was collected. Chl *a* data collected by the CalCOFI program at station 80.100 quarterly from 1981 to 2005 were binned into 10-m depth intervals and analyzed. Open circles are the mean value in each depth interval, and error bars represent the 75th and 25th percentiles.

(Tables 2, 3; Fig. 8A,B). While the effects of iron were usually confined to diatoms in our experiments, pigment data from KN1 indicated that many components of the eukaryotic phytoplankton community displayed responses characteristic of iron–light colimitation in this subsurface chlorophyll maximum, including prymnesiophytes and possibly pelagophytes, in addition to diatoms. This further indicates that the influence of iron was especially strong in this stratum (Fig. 8B). While available data are insufficient to establish the precise cause of the unusually high subsurface chlorophyll maximum biomass at this location, some local process was likely responsible. The observations of strong iron effects and significant changes in community structure in this experiment support our hypothesis that iron availability is likely to be an especially important factor to consider when nutrients are rapidly moved into the lower euphotic zone.

Phytoplankton community responses and environmental relevance—Subsurface chlorophyll maxima phytoplankton communities in the eastern Pacific were quite diverse and contained substantial abundances of cyanobacteria, prymnesiophytes, pelagophytes, and diatoms (Fig. 10A). Effects of iron on net growth rates were generally confined to diatoms, indicating that iron availability, in conjunction

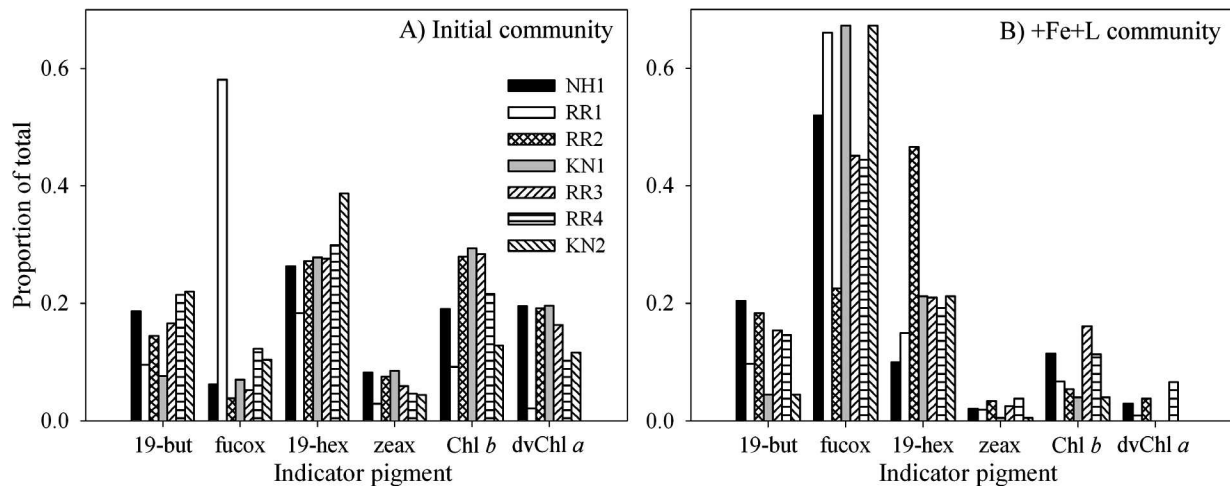


Fig. 10. A comparison of phytoplankton pigment community structure in (A) initial waters collected for incubation and (B) the final +Fe+L community. As a proportion of the total taxonomically informative pigments shown, fucoxanthin increased dramatically in +Fe+L communities compared to the initial community. The initial community at most stations was fairly diverse, as demonstrated by the even distribution of pigments from divergent phytoplankton taxa.

with light, may be influencing their productivity and abundances within many of the SCMs studied. A comparison of pigment distributions in initial SCM phytoplankton communities with +Fe+L treatments showed that relief of iron and light limitations led to dramatic diatom dominance (Fig. 10). Similar shifts to diatom dominance are reflected in comparisons of control and +Fe+L communities. Microscopy and size-fractionated Chl *a* analyses show that these diatoms are large and most commonly dominated by pennate *Pseudonitzschia* and *Nitzschia* species (Fig. 7; Table 5), which often respond to iron addition in other iron-limited regions (de Baar et al. 2005). However, changes in diatom biomass in situ would also likely be influenced by mesozooplankton grazing, which is not adequately represented in microcosm experiments. Additionally, microzooplankton grazing may affect taxa differently in situ in comparison with experimental conditions. Despite these caveats, the strong shift toward diatom dominance suggests that a similar shift, though perhaps of lesser magnitude, could occur in situ when iron and light limitations are relieved.

Because macronutrients, generally nitrogen, control new production in the water columns studied, iron availability would not be expected to affect carbon flux out of the euphotic zone under steady-state conditions (Eppley and Peterson 1979). However, by modifying ecosystem structure, iron could influence the type of material exported and the efficiency of nutrient export relative to recycling (the *f*-ratio). When iron availability is higher, larger diatoms may become more abundant within SCMs, changing the size and taxonomic structure of the phytoplankton community, which would have consequences for ecosystem structure and nutrient cycling. Small phytoplankton are grazed by microzooplankton, routing carbon through the tightly coupled microbial loop where the vast majority of the carbon is remineralized. In contrast, larger phytoplankton have higher sinking rates and are preferentially eaten by metazoan grazers (Michaels and Silver 1988; Boyd and

Newton 1999; but see Richardson and Jackson 2007). By enhancing the growth of large diatoms, iron-induced shifts in size structure could result in more rapid nutrient export at SCMs, where nutrients first enter the euphotic zone, reducing the *f*-ratio of the system (Eppley and Peterson 1979). Additionally, iron availability may modify the type of material exported. In particular, larger diatoms sink more rapidly than much of the SCM phytoplankton community, and potential changes in food-web structure when larger phytoplankton dominate could result in greater production of dense fecal pellets from copepods, leading to deeper carbon export (Michaels and Silver 1988). Iron could even increase the magnitude of carbon flux from the system if its availability mediated increases in the C:N ratio of exported material, since N fluxes generally control new and export production in the eastern Pacific (Behrenfeld et al. 2006). In several experiments, we did observe marked increases in the C:N ratio of particulate matter under iron-replete conditions, suggesting that direct export of this material could result in greater carbon export (see Results). However, whether this increased C:N ratio would be transmitted through the food web to enhance other routes of carbon export is unknown.

In conclusion, these experiments show that iron availability is an important factor structuring SCM phytoplankton communities in macronutrient-limited water columns of the eastern Pacific. Eukaryotic phytoplankton, principally larger diatoms, showed responses to iron and light manipulations suggestive of iron–light colimitation, which may be a consequence of the high iron requirements of photosynthetic-reaction-center and electron-transport proteins. Iron availability affected the taxonomic and size structure of the phytoplankton community, which may have implications for nutrient and carbon cycling within SCMs, where most new nutrients are introduced to the euphotic zone. Influences of iron on SCM phytoplankton communities were observed in both the ETNP and the SCB, suggesting that iron is important in much of the

Pacific where eolian iron supply is low. Low iron concentrations in SCMs in the Sargasso Sea indicate that iron availability may influence lower euphotic zone phytoplankton in the Atlantic as well, but experimental verification of iron limitation remains to be demonstrated (Sedwick et al. 2005).

References

- ANDERSON, R. A., R. R. BIDIGARE, M. D. KELLER, AND M. LATASA. 1996. A comparison of HPLC pigment signatures and electron microscopic observations for oligotrophic waters of the North Atlantic and Pacific Oceans. *Deep-Sea Res. II* **43**: 517–537.
- ARRIGO, K. R. 2005. Marine microorganisms and global nutrient cycles. *Nature* **437**: 349–355.
- BEHRENFELD, M. J., K. WORTHINGTON, R. M. SHERRELL, F. P. CHAVEZ, P. STRUTTON, M. MCPHADEN, AND D. M. SHEA. 2006. Control on tropical Pacific Ocean productivity revealed through nutrient stress diagnostics. *Nature* **442**: 1025–1028.
- BENITEZ-NELSON, C. R., AND OTHERS. 2007. Mesoscale eddies drive increased silica export in the subtropical Pacific Ocean. *Science* **316**: 1017–1021.
- BOWIE, A. R., E. P. ACHTERBERG, R. FAUZI, C. MANTOURA, AND P. J. WORSFOLD. 1998. Determination of sub-nanomolar levels of iron in seawater using flow injection with chemiluminescence detection. *Anal. Chim. Acta* **361**: 189–200.
- BOYD, P. W., A. C. CROSSLEY, G. R. DITULLIO, F. B. GRIFFITHS, D. A. HUTCHINS, B. QUEGUINER, P. N. SEDWICK, AND T. W. TRULL. 2001. Control of phytoplankton growth by iron supply and irradiance in the subantarctic Southern Ocean: Experimental results from the SAZ project. *J. Geophys. Res.* **106**: 31573–31583.
- , AND P. P. NEWTON. 1999. Does planktonic community structure determine downward particulate organic carbon flux in different oceanic provinces? *Deep-Sea Res. I* **46**: 63–91.
- COALE, K. H., AND K. W. BRULAND. 1987. Oceanic stratified euphotic zone as elucidated by ^{234}Th : ^{238}U disequilibria. *Limnol. Oceanogr.* **32**: 189–200.
- CROOT, P. L., AND M. JOHANSSON. 2000. Determination of iron speciation by cathodic stripping voltammetry in seawater using the competing ligand 2-(2-thiazolylazo)-p-cresol (TAC). *Electroanal.* **12**: 565–576.
- CULLEN, J. J. 1982. The deep chlorophyll maximum: Comparing vertical profiles of chlorophyll *a*. *Can. J. Fish. Aquat. Sci.* **39**: 791–803.
- DE BAAR, H. J. W., AND OTHERS. 2005. Synthesis of iron fertilization experiments: From the iron age to the age of enlightenment. *J. Geophys. Res.* **110**: C09S16, doi: 10.1029/2004JC002601.
- DEUTSCH, C., N. GRUBER, R. M. KEY, AND J. L. SARMIENTO. 2001. Denitrification and N_2 fixation in the Pacific Ocean. *Glob. Biogeochem. Cy.* **15**: 483–506.
- EPPLEY, R. W., AND B. J. PETERSON. 1979. Particulate organic matter flux and planktonic new production in the deep ocean. *Nature* **282**: 677–680.
- FENNEL, K., AND E. BOSS. 2003. Subsurface maxima of phytoplankton and chlorophyll: Steady-state solutions from a simple model. *Limnol. Oceanogr.* **48**: 1521–1534.
- FREW, R. D., D. A. HUTCHINS, S. NODDER, S. SANUDO-WILHELMY, A. TOVAR-SANCHEZ, K. LEBLANC, C. E. HARE, AND P. W. BOYD. 2006. Particulate iron dynamics during Fe cycle in subantarctic waters southeast of New Zealand. *Glob. Biogeochem. Cy.* **20**: GB1S93, doi: 10.1029/2005GB002558.
- GEIDER, R. J., H. L. MACINTYRE, AND T. M. KANA. 1998. A dynamic regulatory model of phytoplanktonic acclimation to light, nutrients, and temperature. *Limnol. Oceanogr.* **43**: 679–694.
- GOERICKE, R., AND J. P. MONTOYA. 1998. Estimating the contribution of microalgal taxa to chlorophyll *a* in the field—variations of pigment ratios under nutrient- and light-limited growth. *Mar. Ecol. Prog. Ser.* **169**: 97–112.
- GREENE, R. M., R. J. GEIDER, Z. KOLBER, AND P. G. FALKOWSKI. 1992. Iron-induced changes in light harvesting and photochemical energy conversion processes in eukaryotic marine algae. *Plant Physiol.* **100**: 565–575.
- HAYWARD, T. L., AND E. L. VENRICK. 1998. Nearsurface pattern in the California Current: Coupling between physical and biological structure. *Deep-Sea Res. II* **45**: 1617–1638.
- HERBLAND, A., AND B. VOITURIEZ. 1979. Hydrological structure analysis for estimating the primary production in the tropical Atlantic Ocean. *J. Mar. Res.* **37**: 87–101.
- HOPKINSON, B. M., AND K. A. BARBEAU. 2007. Organic and redox speciation of iron in the eastern tropical North Pacific suboxic zone. *Mar. Chem.* **106**: 2–17.
- HUTCHINS, D. A., G. R. DITULLIO, Y. ZHANG, AND K. W. BRULAND. 1998. An iron limitation mosaic in the California upwelling regime. *Limnol. Oceanogr.* **43**: 1037–1054.
- , AND OTHERS. 2002. Phytoplankton iron limitation in the Humboldt Current and Peru Upwelling. *Limnol. Oceanogr.* **47**: 997–1011.
- JEFFREY, S. W., AND S. W. WRIGHT. 1994. Photosynthetic pigments in the Haptophyta, p. 111–132. *In* J. C. Green and B. S. C. Leadbeater [eds.], *The Haptophyte algae*. Clarendon.
- JOHNSON, K. S., R. M. GORDON, AND K. H. COALE. 1997a. What controls dissolved iron concentrations in the world ocean? *Mar. Chem.* **57**: 137–161.
- , R. M. GORDON, AND K. H. COALE. 1997b. What controls dissolved iron concentrations in the world ocean? Author's closing comments. *Mar. Chem.* **57**: 181–186.
- KING, A. L., AND K. BARBEAU. 2007. Evidence for phytoplankton iron limitation in the southern California Current System. *Mar. Ecol. Prog. Ser.* **342**: 91–103.
- LANDE, R., AND C. S. YENTSCH. 1988. Internal waves, primary production and the compensation depth of marine phytoplankton. *J. Plankton Res.* **10**: 565–571.
- LETELIER, R. M., D. M. KARL, M. R. ABBOTT, AND R. R. BIDIGARE. 2004. Light-driven seasonal patterns of chlorophyll and nitrate in the lower euphotic zone of the North Pacific Subtropical Gyre. *Limnol. Oceanogr.* **49**: 508–519.
- MALDONADO, M. T., P. W. BOYD, P. J. HARRISON, AND N. M. PRICE. 1999. Co-limitation of phytoplankton growth by light and Fe during winter in the NE subarctic Pacific Ocean. *Deep-Sea Res. II* **46**: 2475–2485.
- MCGILLICUDDY, D. J., A. R. ROBINSON, D. A. SIEGEL, H. W. JANNASCH, R. JOHNSON, T. D. DICKEY, J. MCNEIL, A. F. MICHAELS, AND A. H. KNAP. 1998. Influence of mesoscale eddies on new production in the Sargasso Sea. *Nature* **394**: 263–266.
- , AND OTHERS. 2007. Eddy/wind interactions stimulate extraordinary mid-ocean plankton blooms. *Science* **316**: 1021–2026.
- MICHAELS, A. F., AND M. W. SILVER. 1988. Primary production, sinking fluxes and the microbial food web. *Deep-Sea Res. A* **35**: 473–490.
- MILLS, M. M., C. RIDAME, M. DAVEY, J. LAROCHE, AND R. J. GEIDER. 2004. Iron and phosphorus co-limit nitrogen fixation in the eastern tropical North Atlantic. *Nature* **429**: 292–294.

- MOORE, C. M., M. M. MILLS, A. MILNE, R. LANGLOIS, E. P. ACHTERBERG, K. LOCHTE, R. J. GEIDER, AND J. LA ROCHE. 2006. Iron limits primary productivity during spring bloom development in the central North Atlantic. *Glob. Change Bio.* **12**: 626–634.
- PARSLOW, J. S., P. W. BOYD, S. R. RINTOUL, AND F. B. GRIFFITHS. 2001. A persistent subsurface chlorophyll maximum in the Interpolar Frontal Zone south of Australia: Seasonal progression and implications for phytoplankton–light–nutrient interactions. *J. Geophys. Res.* **106**: 31543–31557.
- PRICE, N. M. 2005. The elemental stoichiometry and composition of an iron-limited diatom. *Limnol. Oceanogr.* **54**: 1159–1171.
- , AND F. M. M. MOREL. 1990. Cadmium and cobalt substitution for zinc in a marine diatom. *Nature* **344**: 658–660.
- RAVEN, J. A. 1990. Predictions of Mn and Fe use efficiencies of phototrophic growth as a function of light availability for growth and of C assimilation pathway. *New Phytol.* **116**: 1–18.
- RICHARDSON, T. L., AND G. A. JACKSON. 2007. Small phytoplankton and carbon export from the surface ocean. *Science* **315**: 838–840.
- SAITO, M. A., T. GOEPFERT, AND J. T. RITT. 2008. Some thoughts on the concept of colimitation: Three definitions and the importance of bioavailability. *Limnol. Oceanogr.* **53**: 276–290.
- SCHREIBER, U., H. HORMANN, C. NEUBAUER, AND C. KLUGHAMMER. 1995. Assessment of photosystem II photochemical quantum yield by chlorophyll fluorescence analysis. *Aust. J. Plant Phys.* **22**: 209–220.
- SEDWICK, P. N., AND OTHERS. 2005. Iron in the Sargasso Sea (Bermuda Atlantic Time-series Study region) during summer: Eolian imprint, spatiotemporal variability, and ecological implications. *Glob. Biogeochem. Cy.* **19**: GB4006, doi: 10.1029/2004GB002445.
- STRICKLAND, J. D. H., AND T. R. PARSONS. 1972. A practical handbook of sea-water analysis, 2nd ed. V. 167. Fisheries Research Board of Canada.
- STRZEPEK, R. F., AND P. J. HARRISON. 2004. Photosynthetic architecture differs in coastal and oceanic diatoms. *Nature* **431**: 689–692.
- SUNDA, W. G., AND S. A. HUNTSMAN. 1997. Interrelated influence of iron, light and cell size on marine phytoplankton growth. *Nature* **390**: 389–392.
- TOMAS, C. R. [ED.]. 1997. Identifying marine phytoplankton. Academic.
- VENRICK, E. L. 1998. Spring in the California Current: The distribution of phytoplankton species, April 1993 and April 1995. *Mar. Ecol. Prog. Ser.* **167**: 73–88.
- . 2000. Summer in the Ensenada Front: The distribution of phytoplankton species, July 1985 and September 1988. *J. Plankton Res.* **22**: 813–841.
- WOOD, A. M., D. A. PHINNEY, AND C. S. YENTSCH. 1998. Water column transparency and the distribution of spectrally distinct forms of phycoerythrin-containing organisms. *Mar. Ecol. Prog. Ser.* **162**: 25–31.

Received: 9 July 2007

Accepted: 10 March 2008

Amended: 10 March 2008